PAPER REF: 3019

NON-CONTACT STAND-OFF OPTICAL SENSING OF CABLE VIBRATIONS FOR MONITORING STRUCTURAL HEALTH OF THE WILLIAM H. HARSHA BRIDGE

Jeffrey R. Hay[1], John F. Kielkopf[1(*)], Frank O. Clark[2]
[1]Physics and Astronomy, University of Louisville, Louisville, Kentucky USA 40292
[2]Spectral Sciences Inc., Burlington, MA USA 01803-3304
[(*)]*Email:* kielkopf@louisville.edu

ABSTRACT

We describe a methodology to relate optical signals to surface motion, and apply it to the detection and assessment of bridge structural health. Ambient daylight scattered from a bridge is modulated by bridge motion. When detected with high-dynamic range sensors that possess low intrinsic noise levels, very slight movement in a structure produces measurable intensity level changes in the signal. We have shown in laboratory tests that this intensity level change may be precisely related to the displacement of high contrast features, and may be calibrated against reference measurements with a laser Doppler vibrometer. However, unlike the active illumination of the laser system, passive imaging technology works at very long range and can be used to determine motions of an entire bridge from a convenient stand-off location. When the temporal data are Fourier analyzed, the principal components that appear in the spectrum correlate with the resonant frequencies of the structure excited by urban seismic noise, wind, and traffic. Given a finite-element analysis baseline model, or prior measurement, changes in the modal patterns may be used to determine structural health.

INTRODUCTION

We have developed stand-off optical sensors that detect very small intensity changes caused by motions in large structures such as highway bridges, when stimulated by ambient traffic and seismic background noise. We have shown that analysis of the intensity changes of the optical signals yields displacements over time, and spatial resolution of transient structural resonances (Hay, et al. 2012). The measurements have been validated by *in situ* accelerometers for one test bridge. A system of hardware and software has been built that enables the rapid non-contact assessment of the structural characteristics of bridges using ambient light from a distance. This paper details the results of field studies of three bridges in the United States: the Eastern Parkway (U.S. 60) overpass of the CSX railroad at the University of Louisville, the Sherman-Minton Bridge over the Ohio River at Louisville, Kentucky, and the William H. Harsha Bridge over the Ohio River at Maysville, Kentucky. Finite element analyses of the Eastern Parkway bridge and the William H. Harsha bridge reveal the same or analogous resonances as were detected optically. *In situ* accelerometer measurements made over a long time span are also consistent with the optical measurements. We show how the optical system is capable of detecting theoretically expected modal patterns not usually observable in the field. This paper documents the data collection and analyses completed as of 15 January 2012.

SYSTEM COMPONENTS

The components of the sensor system used for this work are:

- Panasonic CF-30 Toughbook portable computer
- National Instruments 9234 -channel 24-bit +/- 5 V AC/DC analog to digital converter with a 9162 USB interface
- Crossbow CXL02TG3 +/- 2 g low-noise tri-axial precision accelerometer
- Celestron Power Tank 12 VDC portable power supply
- Celestron Onyx 500 mm focal length, f/6.25 ED achromatic telescope
- Meade Optical flip-mirror Model 647
- Fiber-optically coupled near-infrared (1.6 micron) InGaAs photodiode
- Proprietary transimpendance high-gain low-noise amplifier
- Allied Vision Technologies F032B Pike Firewire video camera
- Tamron 16 mm and 50 mm focal length f/2.8 machine vision camera lenses
- SIIG Firewire 800 cardbus interface
- Proprietary LabVIEW and StreamPix5 software

For a single element photodiode, the telescope focuses an image of the bridge on a fiber optic that carries light to the optical sensor. The photodiode has a dynamic range of 1,000,000:1 providing sensitivity for small motions while sampling a single region 5 cm across on a bridge element 200 meters away. For the video camera, a 16 mm lens focuses the scene on an imager with 640x480 elements, each element sampling 9 cm at the same distance, covering a field of view 58x43 meters. The lens and video camera allow rapid surveys of motion, while the single photodiode provides precise localized measurements. An accelerometer is used for *in situ* verification and monitoring.

CSX EASTERN PARKWAY OVERPASS

The CSX main railroad line overpass on Eastern Parkway (US 60) at the University of Louisville in Louisville, Kentucky USA, is a reinforced concrete arch bridge that was known to be structurally deficient at the time our project began. Within months of the initiation of our study, the Kentucky Transportation Cabinet awarded a contract for reconstruction of the bridge, which began in August 2010. We were allowed to locate a wired accelerometer on the bridge deck underside that remained in place and provided nearly continuous monitoring for 2 years while we tested, improved, and calibrated the optical sensor technology.

In this paper, we draw a comparison between accelerometer measurements, optical measurements, and a finite element analysis (FEA) for the Eastern Parkway Bridge that incorporates the long term accelerometer monitoring data, selectively placed accelerometer measurements, and remote stand-off optical measurements. We show that all of these signals are consistent with the FEA for this concrete structure.

Figure 1. Eastern Parkway Bridge over the CSX main line in February 2008 before reconstruction. Pier 1 is the first pier at the near (west) end in this view.

The Eastern Parkway US 60 concrete bridge over the CSX main railway line is adjacent to the University of Louisville campus. A photograph taken in February 2008 is shown in Figure 1. The bridge is a series of arched segments, each of 8 parallel beams 6.5' apart supporting a roadway deck. (Kentucky Department of Highways 2009) Each segment is supported by piers that are sequentially numbered from 1 to 14, starting at the west end seen in Figure 1. The structure is detailed in the engineering drawing of Figure 9 below. From the west, the solid deck spans from the abutment to Pier 4 where there is an expansion joint. Another section continues from Pier 4 across CSX to Pier 9. The third section is from Pier 9 to the east abutment. There are neoprene expansion dams over Piers 4 and 9, where spans join.

Figure 2. Piers 3, 4, 5, ..., looking east at Brook Street, showing deterioration of the concrete prior to reconstruction.

Figure 3. Cracked concrete in abutment at the northwest end of the bridge prior to reconstruction.

Figure 4. Reconstruction of Pier 5. A monitoring tri-axial accelerometer was located under the north center beam midway between Piers 5 and 6.

Figure 5. Pier 4 during reconstruction. The deck was supported by temporary steel I-beams.

Figure 6. A new concrete cap was cast in place over the rebuilt piers.

Figure 7. With forms removed, the stepped support is visible in this side view of Pier 4, where two independent arch sections meet at an expansion dam.

Figure 7 shows the reconstruction work on Pier 4. At other piers the deck may be pinned or free to move, design elements that are incorporated in the models and would affect the response of the structure to load and stimulation by urban seismic noise. Although these spans are not tightly coupled to one another, they are complex structures that are expected to have unique resonances that may differ slightly from one another.

Figure 8. Eastern Parkway Bridge over the CSX main line in January 2012 after reconstruction.

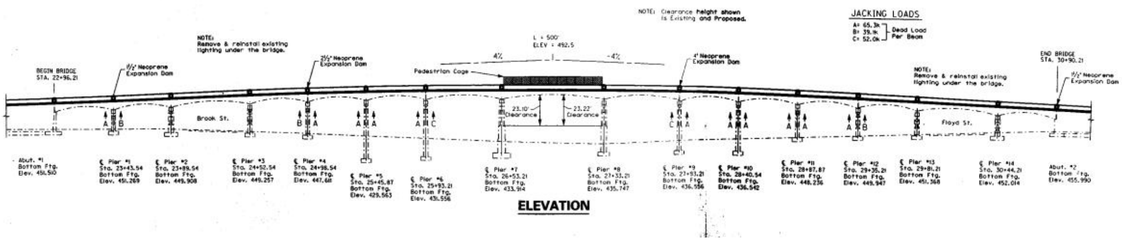

Figure 9. Engineering plan for reconstructed Eastern Parkway Bridge. Pier 1 is the first on the left. Expansion dams are over Piers 4, 9, and 15. (Kentucky Department of Highways 2009)

We measured the motion of this bridge with continuous monitoring by the tri-axial accelerometer fixed to the bottom of a girder midway between Piers 5 and 6. This monitor was in operation from September 2009 through November 2011 and included the period when the bridge was reconstructed through its reopening on 22 June 2010. Samples covering one day shown as "waterfall" or spectral images are in Figure 10. In each image one hour is shown left-to-right, and frequencies from DC to 50 Hz are shown bottom to top. One picture element, or pixel, covers 1 second x 1 Hz in each image. A horizontal band represents a characteristic frequency, and a vertical band an event that stimulated the motion. The diurnal traffic pattern and the start/stop pattern of traffic control is apparent. The bridge shows a fundamental vibration at approximately 6 Hz. The second harmonic at 12 Hz is prominent.

On 11 November 2010, we made stand-off optical detection and *in situ* acceleration measurements on the bridge span over CSX. The methodology has been described previously. A spectral image from the accelerometer is shown in Figure 11. The data shown are similar to those from the permanent accelerometer, but on a shorter time span of 360 seconds that resolves distinct events. The 6 Hz resonant frequency seen in the accelerometer data above between Piers 5 and 6 is also apparent here, and the 12 Hz second harmonic is strong. There is a broad 30 Hz feature that appears when the span is strongly excited, and a narrow structure that starts at above 50 Hz and rapidly decreases to below 30 Hz in the last minute of data. Clearly some features are due to ambient events not associated with the bridge, but the correlation with time apparent in the figure is a clue indicating the origin of the signals. Similarly, when an image is available, correlation in space across a structure may be used to localize vibrations spatially.

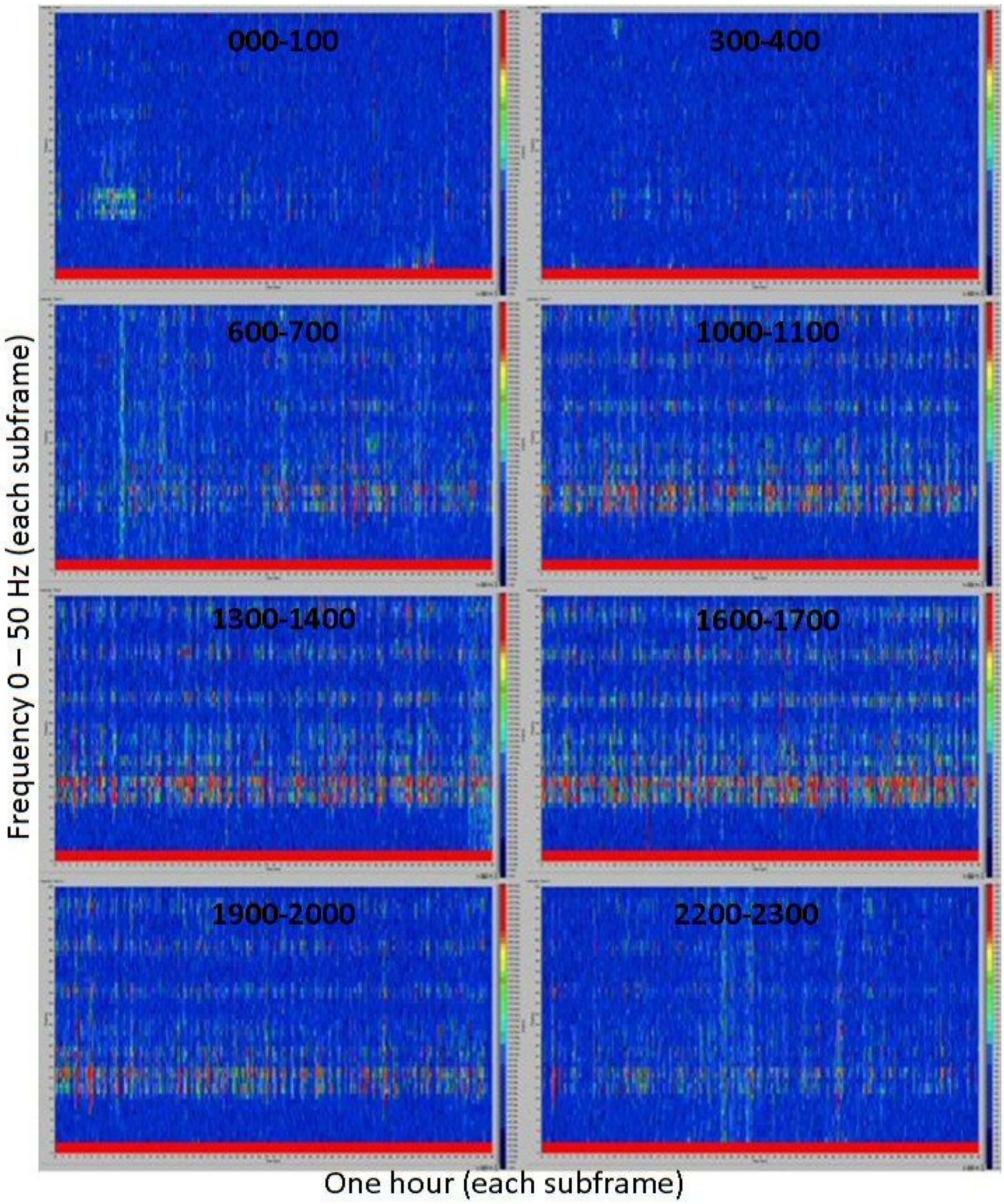

Figure 10. Accelerometer data of the 5-6 span on 10 January 2011. Left to right, then top to bottom 0000-0100 Eastern Standard Time (EST), 0300-0400, 0600-0700, 1000-1100, 1300-1400, 1600-1700, 1900-2000, 2200-2300. Each image shows frequencies from 0 (bottom) to 50 Hz (top) for 1 hour from left to right. Red indicates strong motion.

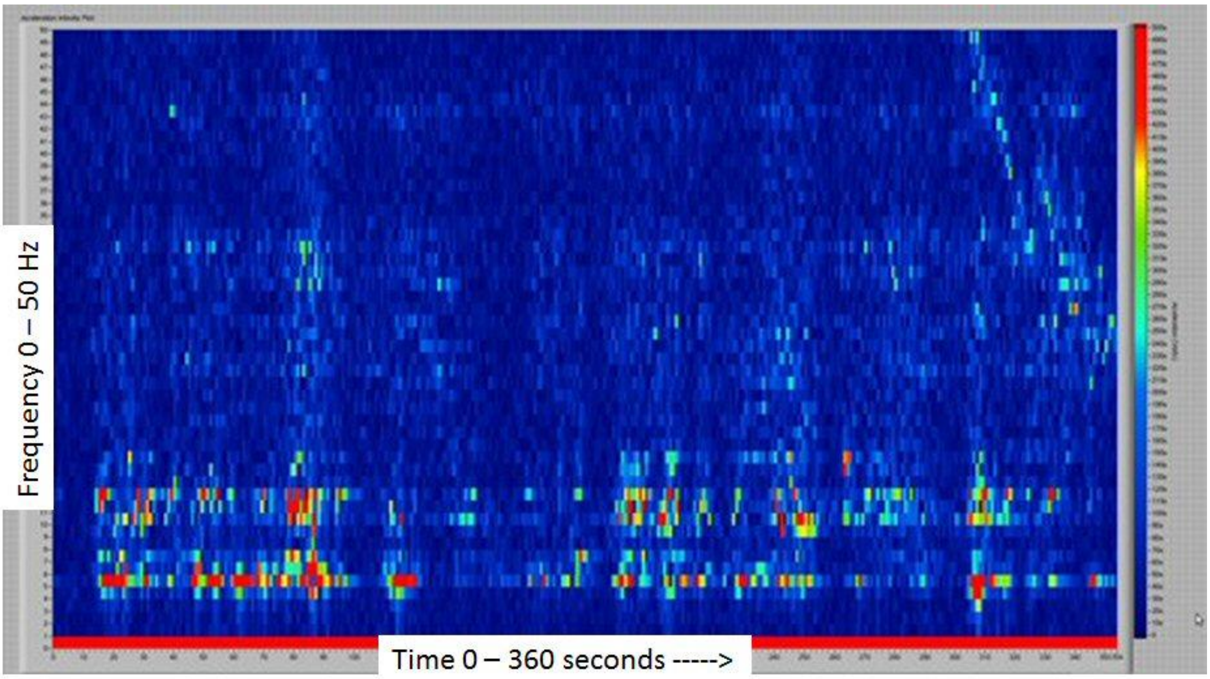

Figure 11. A spectral image of vibrations measured with an accelerometer on the deck of the Eastern Parkway Bridge between Piers 7 and 8. The data were recorded on 18 November 2010. 1530 EST, simultaneously with optical measurements taken from the ground nearby. The strong low frequency resonance is at 6 Hz.

Plots of the acceleration data from a 12 second interval when a bus passed over the arch are shown in Figures 12 and 13. In Figure 12 we show the Fourier analysis of the signal relative to DC, scaled so that at each frequency the amplitude of the principal component is given in units of "g", the acceleration of gravity (9.8 m/s^2 or 980 cm/s^2). For a harmonic oscillator at frequency f, the amplitude of the periodic motion z (perpendicular to the deck) over time t, is $z_0 \sin(2\pi\ ft)$. The acceleration is $a = z_0\ (2\pi\ f)^2 \sin(2\pi\ ft)$, meaning that for a given motion the accelerations are scaled by the square of the frequency. For this reason the accelerometer measurements weight high frequencies heavily. We reduce a measurement of acceleration to displacement by dividing by $(2\pi\ f)^2$. The result for these data are shown in Figure 13.

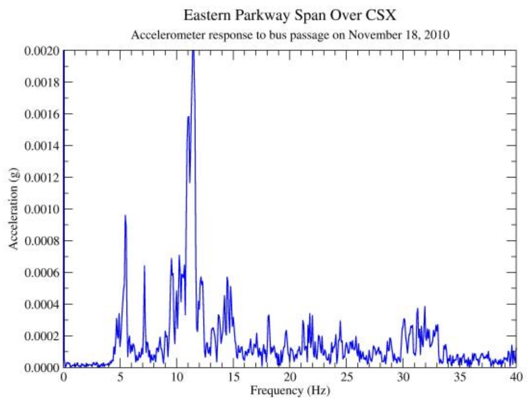

Figure 12. Accelerations of the span between Piers 7 and 8.

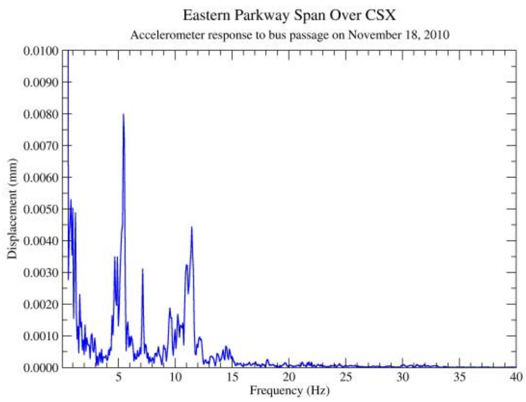

Figure 13. Displacements derived from the measurements of acceleration on the CSX span.

The simultaneous optical measurements for this span are shown in Figure 14. These were made with a 50 mm focal length lens and the single-element photodiode sensor in order to obtain the highest possible signal-to-noise with large dynamic range. The optical sensor detected at a distance exactly the same frequencies seen with an accelerometer on the deck.

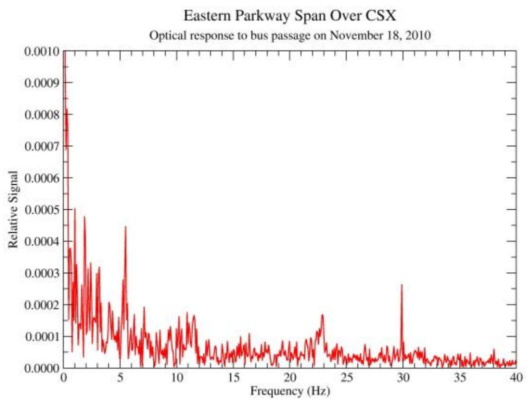

Figure 14. Optical measurement of the resonant frequency of the Eastern Parkway bridge span over the CSX tracks, between Piers 7 and 8. Compare to the displacement derived from the accelerometer measurements in Figure 13.

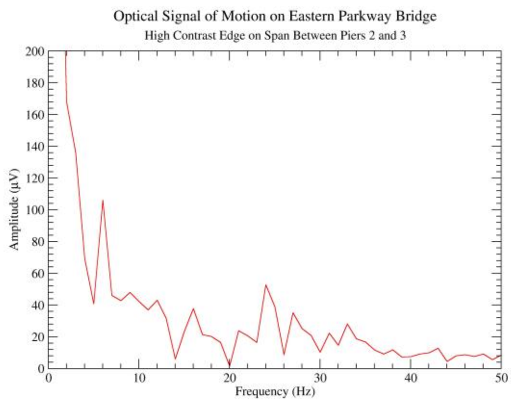

Figure 15. Optical measurement of the frequencies in the span between Piers 2 and 3. The 6 Hz resonance is clearly detected above a complex background of seismic noise and possibly other modes of bridge motion.

Other optical measurement of the resonances made on different occasions and for other spans are shown in Figures 15 and 16. There is a consistent pattern, with the 6 Hz resonance almost always seen in sensitive optical detection, and the 6 and 12 Hz features seen in the accelerometer data. A systematic exploration of the bridge with an accelerometer showed evidence of a possible small shift in the resonance with section, symmetric about the center of the structure, but this detail needs further investigation and analysis.

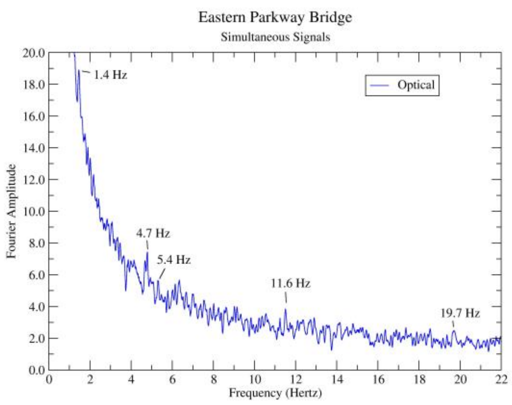

Figure 16. Optical measurement of the frequencies in the span between Piers 8 and 9 east of the CSX tracks. Longer time span data sharpen the persistent resonances but increase background to signal since the stimulating events are of short duration.

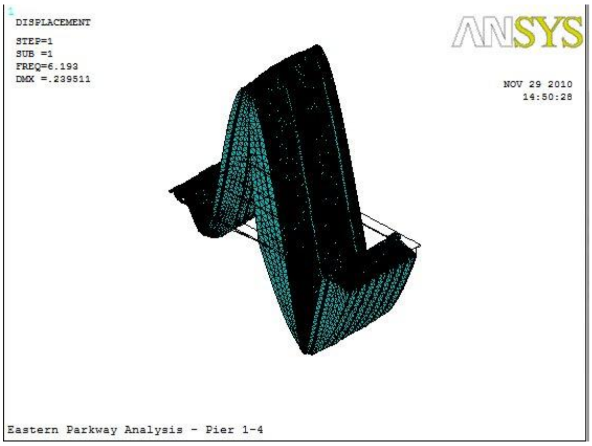

Figure 17. A 6.2 Hz resonance in the first (western most) span between Piers 1 and 4. The figure illustrates the exaggerated displacement of the vertical motion from equilibrium. (Perez 2011)

A finite element analysis of the bridge was undertaken by Christina Perez, a graduate student working with Prof. J.P. Mohsen in the Department of Civil Engineering of the University of Louisville. (Perez 2011) Their unpublished dynamic analysis using Ansys revealed a resonant mode shown in Figure 17 with a frequency of 6.2 Hz.

The structural analysis leading to the discovery of the mode showed static displacements of the deck resulting from its own weight, and the changes in those displacements as they would occur under load. The optical sensors are capable of measuring static as well as dynamic displacements but we have focused here on the use of time domain data.

SHERMAN-MINTON BRIDGE

The Sherman-Minton Bridge carries Interstate 64 over the Ohio River at Louisville, Kentucky USA. It is a through-arch design using a symmetric pair of steel arches and paired cables to support a double deck below. The arch is under compression while the tie beams of the deck and the suspending cables are under tension. The bridge was found to have significant structural failure of the beam tension members in the fall of 2011. The failure was not identified in bridge inspection reports prior to the bridge's emergency closure, and engineering details of the failure have not been made available to the public. However, we show that the stand-off technology enables a measurement at a safe distance of not only the resonant frequencies in the supporting cables but also their resonant modes. Since the frequency is determined by the loading and the structural integrity of the cabling, these measurements show how remote sensing can be used to assess structural health of components that are subject to critical failures.

Figure 18. A panoramic view of the Sherman-Minton Bridge from the north (Indiana) bank of the Ohio River. The photograph was taken while inspections were underway after the bridge was found to have a critical structural failure.

Figure 19. Attachment of the cables (show to the right in Figure 20) to the arch of the Sherman-Minton Bridge. (Indiana Dept. of Transportation 2009)

Figure 20. Looking down on the attachment of the cables to the tie beam of the Sherman-Minton Bridge. The cables are connected to the arch above (Fig. 19). (Indiana Dept. of Transportation 2009)

Figure 21. Sherman-Minton Bridge seen from an upstream location on the Indiana Bank. The telescopic optical system is shown with the fiber-optically coupled single-element sensor.

Figures 19 and 20 (appropriately rotated), taken from the last available inspection report, show both the state of repair and how the cables are attached to the tie beams. (Indiana Dept. of Transportation 2009) The weight of the deck is supported by two cables on each side. The lower cable ends are free to swing with the deck, while the upper ends are fixed at the arch. The cables behave like a classic vibrating string with a node forced at the arch. A failure in the attachment at the deck which is constantly in motion, or a change in the loading due to a failure in the tie beam, could cause structural collapse if the loading were no longer distributed symmetrically.

We measured the cable resonances with the stand-off optical system from a convenient point on the north bank of the Ohio River, 245 meters upstream from the bridge. The sight line to the center of the bridge was approximately 300 meters. Given this long distance, we used a 16 mm lens with a video camera so that many cables could be monitored simultaneously. The telescopic system with a single element sensor was also employed, as shown in Figure 21, to search for local vibrations in other components. The data acquisition software recorded a 14-bit video image of the bridge, stored in 16-bit arrays, at 107 frames per second. A typical analysis screen is shown in Figure 22.

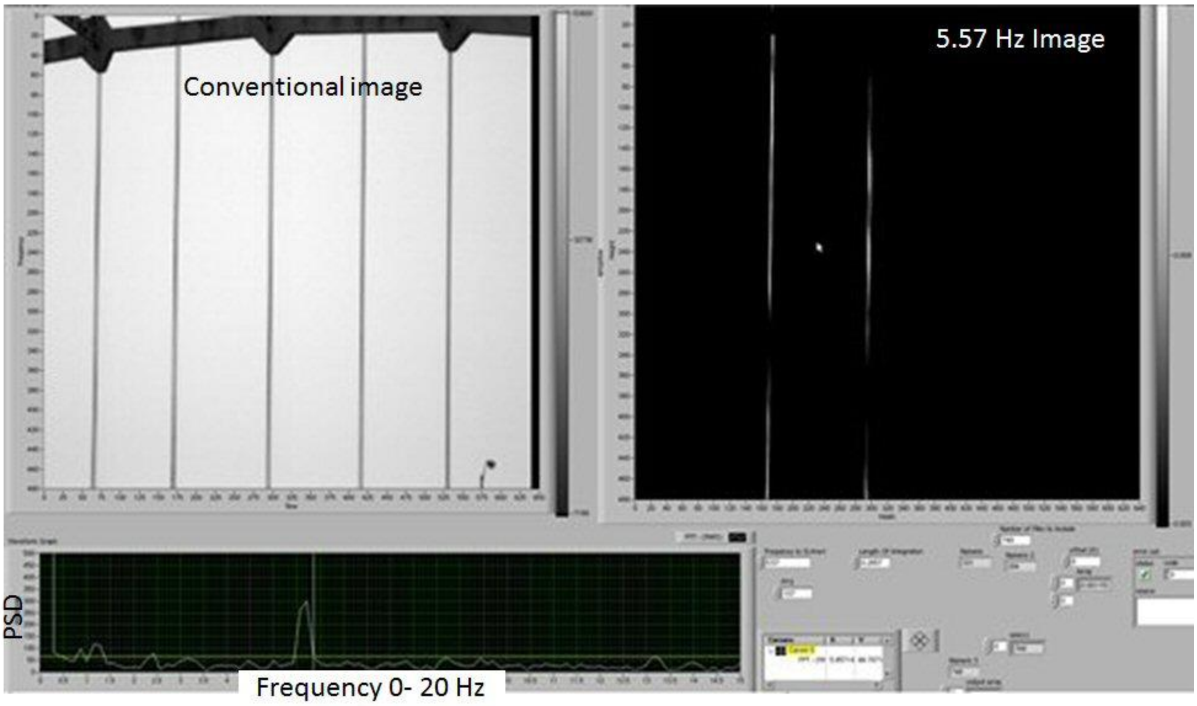

Figure 22. LabVIEW data analysis screen of the Sherman-Minton Bridge taken 14 September 2011.

On the left panel of Figure 22, the video image shows the cable pairs of the north arch. The right panel shows only the features of the image that are vibrating at 5.57 Hz, and the lower graph is the frequency spectrum of a selected cable. We see that by isolating unique frequencies in the Fourier image we can identify individual cables, each with their own distinct resonance. The detection in the Fourier or frequency image shows brightness in proportion to the amplitude of the motion at that frequency, and as a result the image of each cable clearly identifies the location of the nodes (no motion) which appear darker.

The analysis screen allows the selection of a single pixel in the scene from which the temporal data are transformed to produce a frequency spectrum. It accepts a request for a specific frequency, and displays the image of the scene showing only those features that are moving at that frequency. The brightness of the displayed image, shown in the panel on the right, is proportional to the amplitude of the motion. In this figure one may clearly see that the cables on opposite sides of the bridge serving the same functional role have identical frequencies, in this case 5.57 Hz. The nodal pattern is visible in both also, and appears to be same for the upstream and downstream sides.

The power of the method becomes apparent when we compare the view in different frequencies. As shown in Figure 22, the 5.57 Hz view selects only one set of cables serving identical roles. In Figures 23 we can compare two slightly different frequencies to see the effects of loading and cable length.

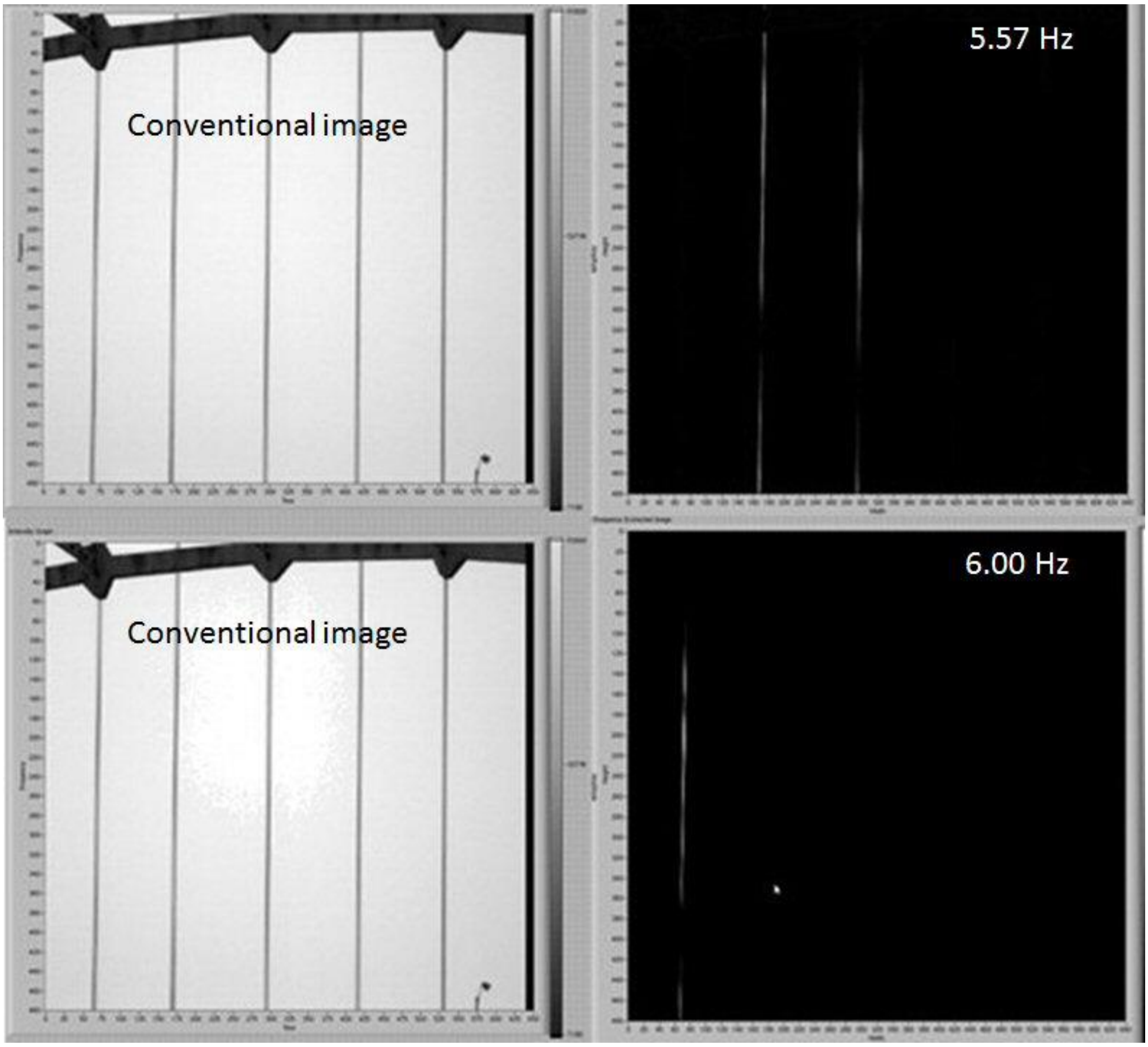

Figure 23. An analysis of video data taken on 14 September 2011. On the left are conventional images. On the right are the images of motion at selected frequencies: 6.00 Hz below and 5.57 Hz above.

Video data work very well with high contrast features such as cables, especially for the large amplitudes of motion that occur on this bridge. As may be seen in figure 23, cables with frequencies that differ by only 0.43 Hz can be distinguished.

To measure the southern arch, the optical system was located on the opposite bank, collecting data diagonally across the river. A view from Google Maps is shown in Figure 24. The sight line was 466 meters, yet even with this long distance the frequencies could be measured accurately and the nodes located. Figure 25 is the analysis screen for the 5th cable pair from the southern bank, on the downstream side of the bridge (left side in the Google view).

We can measure the relative amplitude of the vibration as a function of distance along the cable by determining the strength of the signal in the Fourier image. These data are extracted over a short time span to create a map of the motion averaged over that time. The result is shown in Figure 26.

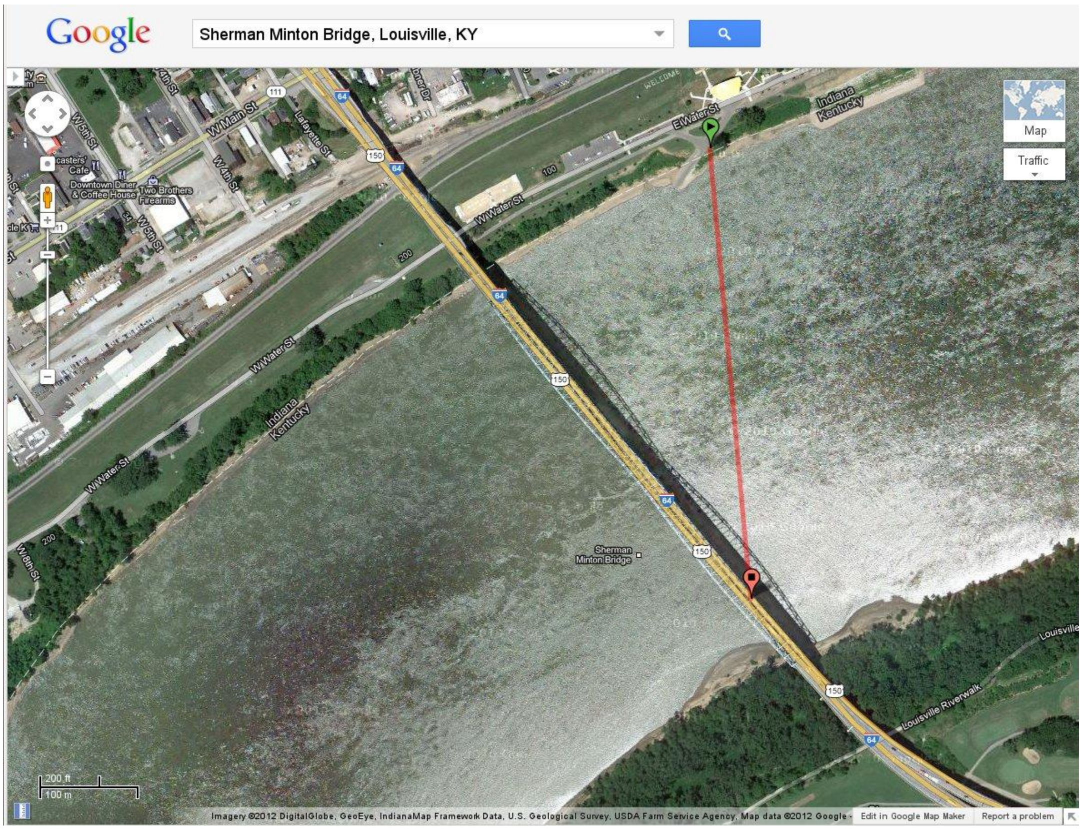

Figure 24. Google Maps view of the location of the video sensor that was used to measure cable resonances. The 466 meter sight line shown is to the 5th cable from the southern bank.

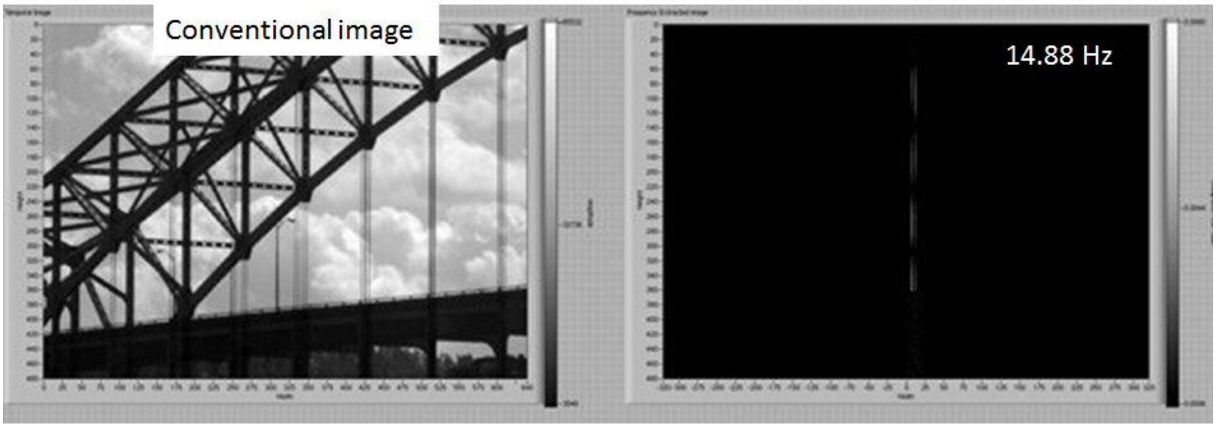

Figure 25. The southern side of the bridge is shown in a conventional single frame from the video data. A Fourier image of the downstream cable 5 pair is in the right frame, processed to show only 14.88 Hz. The cable of interest has been centered.

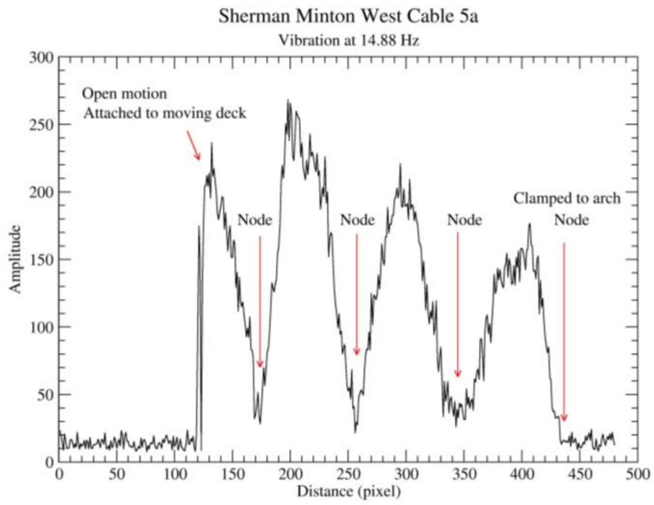

Figure 26. Amplitudes of vibration at 14.88 Hz in one of the cables that make the 5th pair on the southern downstream side of the Sherman-Minton Bridge.

We have noted the positions of the nodes, where motion is minimized. The attachment point on the tie beam (Figure 20) is an antinode with large amplitude motion. It contrasts with the arch (Figure 19) which is a node. This pattern is clearly apparent in the graph shown in Figure 26. The frequencies and nodal pattern are determined by the loading on the cables and their anchoring to the bridge structure. (Chen and Petro 2005)

WILLIAM H. HARSHA BRIDGE

The Maysville, Kentucky USA, William H. Harsha cable-stayed bridge over the Ohio River was opened to traffic in 2001. At that time a comprehensive study was made that included FEA analyses, and *in situ* accelerometer measurements of resonances in supporting cables (Harik et al. 2005). Free vibrations of the cables were determined on three occasions in those studies, and included stimulating motions with loaded trucks, and using ambient traffic and wind. Each test took approximately 1.5 days to survey the bridge. Tests performed when the bridge was first opened differed slightly from those done 5 and 8 months later, and changes were ascribed to breaking-in of castings and to temperature variations. On 5 November 2011, we made stand-off optical measurements of resonant frequencies in a sequence of cables easily visible from the Kentucky shore in order to validate the stand-off passive optical technology, and to assess changes in the bridge that have occurred during 10 years of use. Since a cable-stayed bridge may be surveyed optically from only a few locations on shore, sensors are not attached to the cables, and ambient sources provide adequate stimulation, the standoff system requires only a few hours to develop data equivalent to the prior accelerometer-based survey. Views of the bridge and the optical sensor are shown in Figure 27.

Figure 27. William H. Harsha cable-stayed bridge over the Ohio River at Maysville, Kentucky. The telescope and fiber-optically coupled sensor are shown on the right.

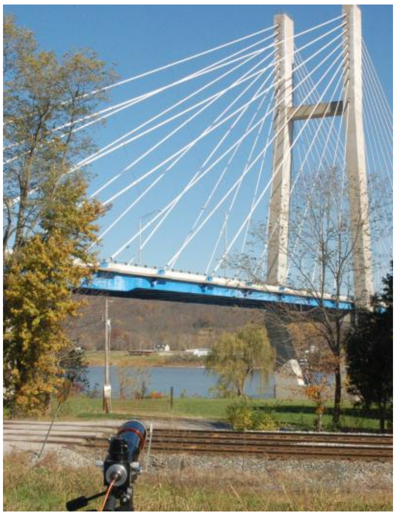

Figure 28 shows a measurement of one of the cables. The resonance is sharply defined and stands out clearly above a background that may include other modes of vibration, coupling from other bridge components, and atmospheric effects. We surveyed several cables in this way, and the data for them are presented in Figure 29 and Table I.

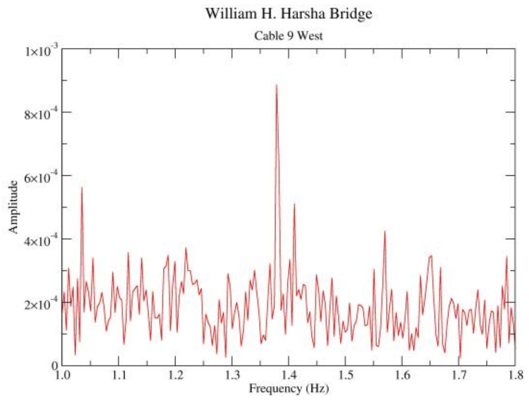

Figure 28. An optical measurement of the resonant frequency of cable 9 on the downstream side of the William H. Harsha bridge.

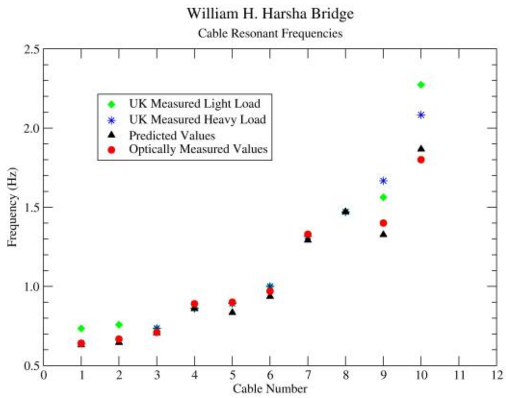

Figure 29. Cable resonant frequencies in the William H. Harsha bridge. The data indicated as UK are from Harik, et al, (Harik 2005) a report to the Kentucky Transportation Cabinet.

RESULTS

Table I below also shows a comparison of the optical and accelerometer data, and the finite element analysis of the structure. The cables are numbered sequentially from the south (Kentucky) end, the bank from which the optical measurements were made. The measurements provided are on the downstream (west) side of the bridge.

Table I: William H. Harsha Bridge

Dominant Resonant Frequency (Hz)

Cable	Accelerometer	Accelerometer	FEA	Optical
	Light Load [1]	Heavy Load [1]	[1]	This Work
1W	0.735	0.641	0.631	0.641
2W	0.758		0.645	0.667
3W	0.735	0.735	0.706	0.71
4W	0.862	0.862	0.860	0.89
5W	0.893	0.893	0.834	0.90
6W	1.000	1.000	0.936	0.97
7W	1.316	1.316	1.292	1.33
8W	1.471	1.471	1.471	
9W	1.563	1.667	1.326	1.40
10W	2.273	2.083	1.666	1.60

The agreement and consistency of the pattern show that the optical method is a reliable and fast alternative to *in situ* accelerometers. Interestingly, the optical measurements follow the FEA closely, and differ from the measurements made 10 years earlier primarily in the longest cables that also showed aging effects in the first few months after construction.

CONCLUSIONS

We have reported here on studies of three types of bridges for which we have either a finite element analysis or an engineering model. For all three we find a correspondence of the expected behavior based on design parameters and the measurements of resonances:

- Eastern Parkway stressed concrete overpass of the CSX railroad exhibited a 6 Hz resonance in the vertical motion of the bridge deck. The optical signal was verified by *in situ* accelerometers at many locations on the deck in short term monitoring, and at a single location monitored for two years. The 6 Hz mode was identified in an FEA model.
- Sherman-Minton through-arch steel bridge over the Ohio River exhibited resonances in the cables from the arch to the tie beam. The cable resonances showed the expected symmetry. The optical measurements revealed the nodal structure, which could be compared with a detailed analysis if structural parameters were known. The symmetry provides a baseline for long term health monitoring.
- William H. Harsha cable-stayed bridge over the Ohio shows exactly the same cable frequencies measured 10 years ago with *in situ* accelerometers, in agreement with a prior FEA model done for the Kentucky Transportation Cabinet.

Most bridges may be thoroughly surveyed optically from only a few stand-off locations. Attached sensors are not required and ambient sources such as traffic, wind, water or even seismic "noise" provides adequate stimulation. The optical technology offers a simple direct way to determine structural resonances. Finite element analyses provide a connection between these measurements and the design of the bridges. Alternatively, baseline comparisons either through construction symmetry or long term database management capture changes due to aging and structural failure. Imaging sensors not only can replace accelerometers for such measurements, but provide information on modal patterns that are not available from single-point accelerometry. The working range of a passive optical system such as described here exceeds that of laser-based velocimetry by at least an order of magnitude.

With high dynamic range temporal imaging, a Fourier transform of each pixel yields a frequency data cube in which each slice is an image of the bridge at the corresponding frequency. The unique resonant frequencies of each individual cable of the through-arch bridge we studied were highlighted in such slices. Nodes in their vibrational pattern were dark, and antinodes bright, thus identifying modes. Used in this way, imaging in the frequency domain is a powerful analysis tool providing more information than discrete accelerometer samples. Identification of bridge structural damage using resonant frequencies is a potentially powerful inspection tool when supported by baseline measurements and validated FEA models. (Ren and Roeck 2002, Lee and Yun 2006) Accelerometer measurements are laborious and expensive. Optical measurements can be made by a technician working safely from a distance in only a few hours. (Hay, Kielkopf, Naber, and Clark, 2012)

ACKNOWLEDGMENTS

The authors acknowledge support from the US Department of Homeland Security, through contracts to the National Institute of Hometown Security. Frank O. Clark acknowledges internal support by Spectral Sciences, Inc.

REFERENCES

Chen, S.-E. and Petro, S., Nondestructive bridge cable tension assessment using laser vibrometry, Experimental Techniques, 29, 29-32, 2005.

Harik, I.E., Hu, J., Smith, S.W., Ren, W.-X., Zhao, T., and Campbell, J.E., Baseline modeling of the Maysville cable-stayed bridge over the Ohio River, Research Report to the Kentucky Transportation Cabinet, KTC-05-10/FRT104-00-1F, Kentucky Transportation Center, July 2005.

Hay, J., Kielkopf, J., Naber, J. , and Clark, F. O., 2012 in preparation.

Indiana Department of Transportation, Bridge Inspection Report, NBI Number 034520, Bridge Number I64-103-04691 C, Facility Carried I-64, 1 October 2009.

Kentucky Department of Highways, Jefferson County Eastern Parkway over CSX Railroad and Floyd Street, Document 1050.0, April 2009.

Lee, J. J. and Yun, C. B., Damage diagnosis of steel girder bridges using ambient vibration data, Eng. Struct. 28, 912-925, 2006.

Perez, Christina, unpublished, 2011.

Ren, W.-X., and De Roeck, G., Structural damage identification using modal data, J. Struct. Eng. 128, 87-95, 2002.